

Scaling Spectral Analysis: A New Tool for Interpretation of Gravity and Magnetic Data

A.R. Bansal and V.P. Dimri

National Geophysical Research Institute, (CSIR)
Hyderabad- 500606

Email: abhey_bansal@ngri.res.in; director@ngri.res.in

Abstract

The scaling spectral method for gravity and magnetic data is found useful for finding the depth values and statistical properties of the source distribution. The depth values calculated by scaling spectral method are close to the realistic values whereas white noise assumption of sources results in overestimations. The scaling spectral method has been applied to many parts of the world. The power spectrum corresponding to low wavenumber may be dominated by scaling properties alone rather than the depth values. The scaling distribution is useful for gridding the datasets, delineating the lithological units and enhancing the information of sources. The long non-stationary profiles and larger areas may be divided into piecewise stationary profiles before applying the scaling spectral method. The values of scaling exponents from the field as well source indicate 3- D distribution of susceptibility and density.

Key Words: scaling spectral method, gridding the datasets, delineating the lithological units, susceptibility, density

Introduction

The interpretation of gravity and magnetic data generally carried out in the space and frequency domains. The interpretation of the gravity and magnetic data is preferred in frequency domain because of simple relation between various source models and field (Naidu and Mathew 1998). The estimation of the depth of anomalous sources is usually carried out by Spector and Grant (Spector and Grant, 1970) method and its variants in frequency domain (Bhattacharyya, 1966; Naidu, 1968; Spector and Grant 1970; Treitel *et al.*, 1971; Hahn *et al.*, 1976; Connard *et al.*, 1983). These methods assume different assemblage of sources like statistical ensemble of prisms (Spector and Grant, 1970), white noise of vertical needles with constant magnetization (Naidu, 1972; Hahn *et al.*, 1976), a sandwich model of uniaxially magnetic sheets (Pedersen, 1991), equivalent density layer (Pawlowski, 1994) etc. These methods are in continuous use since their development because of simplicity (Ofoegbu and Hein, 1991; Cowan and Cowan, 1993; Hildenbrand *et al.*, 1993; Gracia- Abdeslem and Ness, 1994). In case of 2-D data radially averaged power spectrum is proportional to $\exp(-2dk)$, where k is wave number, d is depth to anomalous sources.

The assumptions of sources in these methods lead to white noise distribution. The white noise source distribution is assumed because of mathematical simplicity and limited information about the subsurface source distribution. Recent borehole studies from the German Continental Drilling Program (KTB), the Canadian Shield, etc. have shown scaling noise distribution of physical properties rather than white noise distribution (Pilkington and Todoschuck 1990, 1993, 1995; Maus and Dimri

1995, 1996). The power spectrum of scaling noise can be represented as: $P(k) \sim k^\beta$, where $P(k)$, k and β are the power spectrum, wave number and scaling exponent of the source distribution, respectively. The values of scaling exponents indicate the relation between the successive values, a positive value indicate anti-correlated, negative values indicates correlated and zero value corresponds to white noise.

Pilkington and Todoeschuck (1990) have shown that scaling noise models are more suitable for modeling the spatial variation of geophysical parameters. They analyzed six boreholes, three each of 300m depth and 150m depth from Bells Corners, Ottawa, Canada. The data divided into sedimentary and igneous sections for each borehole. The power spectrum of acoustic impedance, resistivity log, density, gamma-ray log, neutron log is calculated using periodogram technique. The values of scaling exponents of density varies from -0.87 to -1.47 for sediments and -0.71 to -1.71 for igneous rocks. In another study of Pilkington and Todoeschuck (1993) the values of scaling exponents are found varying from -1.32 to -1.96 for sedimentary rocks and from -2.08 to -2.72 for igneous rocks. Leonardi and Kumpel (1998) studied the physical properties of the rocks from the KTB borewell data and found the values of scaling exponents between -1.0 to -1.4 for susceptibility and -0.6 to -1.2 for bulk density. Zhou and Thybo (1998) were in the opinion of variation of scaling exponents with depth for the field as well as source distribution. They analyzed the susceptibility data of the KTB super deep main hole and aeromagnetic data over the Southeastern North Sea. The scaling exponent for KTB susceptibility data varies from -0.6 to -2.0 with a decreasing trend with depth. The values of scaling exponents from aeromagnetic data is found -2.3, -1.1 and -0.96 for three different sedimentary basins of different basement depths in the North Sea area (Zhou and Thybo, 1998). The values of scaling exponents may be anisotropic; different in vertical and horizontal directions (Pilkington and Todoeschuck, 1993). Shiomi *et al.* (1997) analyzed well-log data from five deep wells in different tectonic regions in Japan to study the statistical characteristics of P-wave velocity, S-wave velocity and density in the uppermost part of the crust. The three wells are located in sedimentary rocks in the Kanto Plain and two wells are in the Kuju Volcano Group in Kyushu Island. In the Kanto Plain the scaling exponent ranges between -1.1 to -1.3 from the analysis of P-wave velocity and density, whereas the scaling exponent is -1.3 to -1.6 in Kuju Volcano Group for P and S wave velocities and density. This is an indication of less values of scaling exponent in a tectonically stable area as compared to the tectonically active area. Maus and Dimri (1995) found the values of scaling exponent -2.07 to -2.16 over the KTB main hole and -1.8 over the KTB pilot hole from aeromagnetic data. Analysis of marine gravity data of Norwegian Coast has shown that the scaling exponent is -4.5 (Maus *et al.*, 1998). An example of susceptibility log measured in the KTB pilot hole (Fig. 1a) and its power spectrum (Fig. 1b) with the values of scaling exponent is shown in Fig. 1 (Maus and Dimri, 1995). The scaling noise has no characteristic correlation length (Feder, 1988).

Pilkington and Todoeschuck (1993) studied the relation between the scaling exponent due to the 3-D susceptibility distribution and 2-D magnetic field. They found that susceptibility distribution with scaling exponent (α) will produce a magnetic field with scaling exponent ($\alpha-1$). Maus and Dimri (1994) have studied in detail various relationships between the scaling exponents of density and susceptibility distributions and their respective gravity and magnetic fields for different dimensions (Table-1).

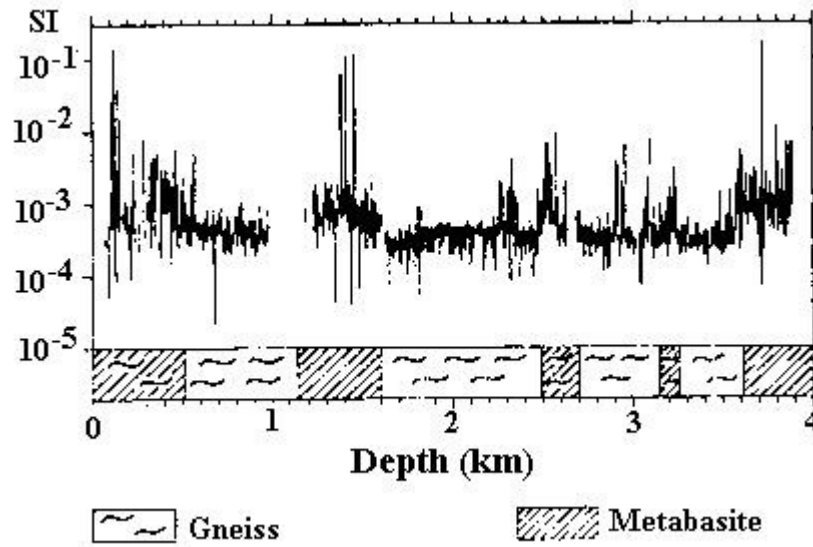


Fig.1 a: Susceptibility log measured in KTB pilot hole with simplified geology (Maus and Dimri, 1995)

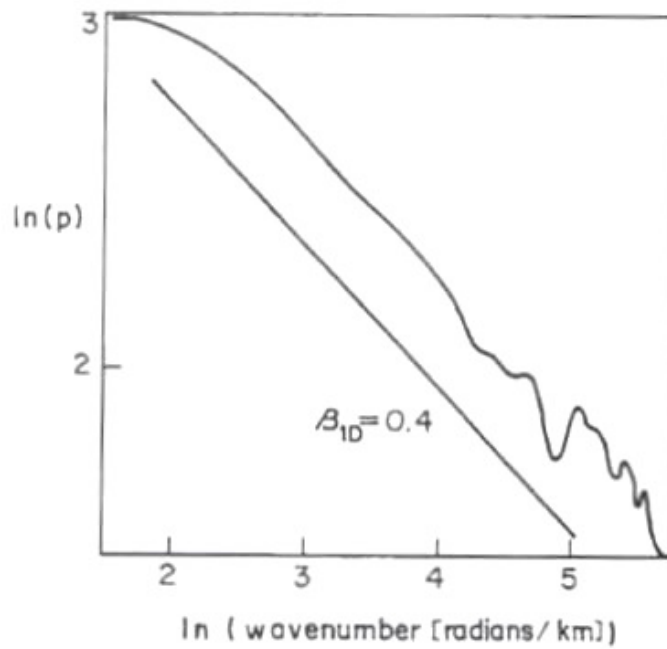


Fig. 1 b: An example of calculation of scaling exponent of the susceptibility log from KTB pilot hole.

Table-1: The relation between the scaling exponent of the density/ susceptibility and gravity/magnetic field in different dimensions (Maus and Dimri, 1994).

	3-D (source)	2-D (source)	1-D (source)	2-D (field)	1-D (field, x, y, z)
Gravity	α	$\alpha-1$	$\alpha-2$	$\alpha+1$	α
Magnetic	α	$\alpha-1$	$\alpha-2$	$\alpha-1$	$\alpha-2$

Calculation of depth values by scaling Spectral Method

The scaling exponent of source distributions can be used as a prior information in term of parameter covariance matrices in linear inversion (Pilkington and Todoeschuck, 1990). Maus and Dimri (1995) suggested the computation of scaling exponents of the field and depth simultaneously from the inversion of power spectrum. In their method power spectrum can be written as:

$$P(k) = Ck^{-\alpha}e^{-2dk} \quad (1)$$

where $P(k)$ is the power spectrum, α is the scaling exponent of the field, k denotes wavenumber, C is a constant depending on the properties of source and d is the depth to the anomalous sources. The parameter α and d are interrelated where lower values of the scaling exponent leads to higher depth and vice versa. The three parameters (C , α , d) can be calculated by the inversion method. The equation (1) may be written in logarithm as:

$$\ln P(k) = C-2dk-\alpha \ln k \quad (2)$$

Although Maus and Dimri (1995, 1996) developed the methodology for half space model, the equation (2) can be applied to the multilayer cases with constant values of scaling constant (Fedi *et al.*, 1997).

Applications

Pilkington and Todoeschuck (1990) used the scaling covariance model in the inversion of DC resistivity sounding data. The use of scaling noise covariance model resulted in reduction of the posteriori parameter variances and smoothness of the solution. The value of scaling exponent from aeromagnetic data over the Canadian Shield is found as -3 (Gregotski *et al.*, 1991). The value of scaling exponent -3 is also found from 2-D susceptibility data for the Sierra Nevada Batholith, California and Flin Flon- Snow Lake Belt, Saskatchewan Island Arch. Canada (Pilkington and Todoeschuck, 1995). This value is a representation of 3-D crustal susceptibility with scaling exponent of -4 (Pilkington and Todoeschuck, 1995). The use of scaling exponent values in deconvolution of aeromagnetic data of northeastern Ontario, Canada result in enhancing the magnetic field anomalies and delineating the litological units (Gregotski *et al.*, 1991). Pilkington *et al.*(1994) studied aeromagnetic

data from Wollaston Lake and Athabasca Sedimentary Basin in the Canadian Shield. In the Wallston Lake area sources are exposed and depth to magnetic sources is corresponds to the flight altitude of 300m whereas in Athabasca

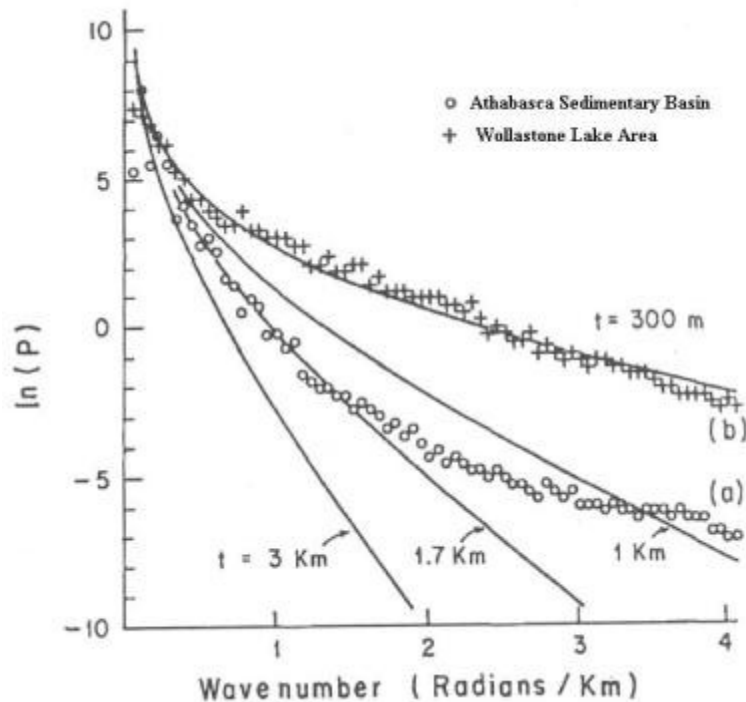


Fig. 2: Radially averaged power spectrum versus wavenumber of aeromagnetic data over the Athabasca sedimentary Basin (a) and Wollastone Lake area (after Maus and Dimri, 2006).

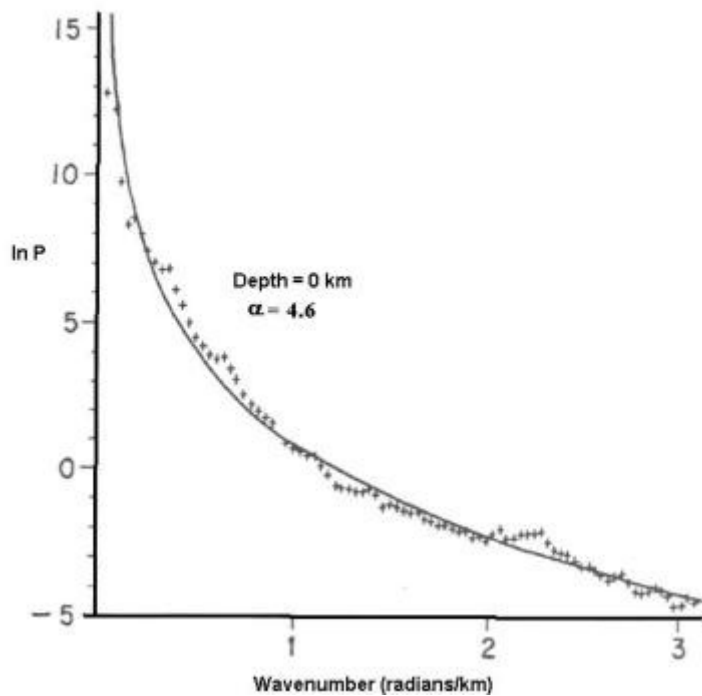


Fig. 3: Depth estimation by scaling spectral method from gravity data of the Paradox Basin(after Maus and Dimri, 2005).

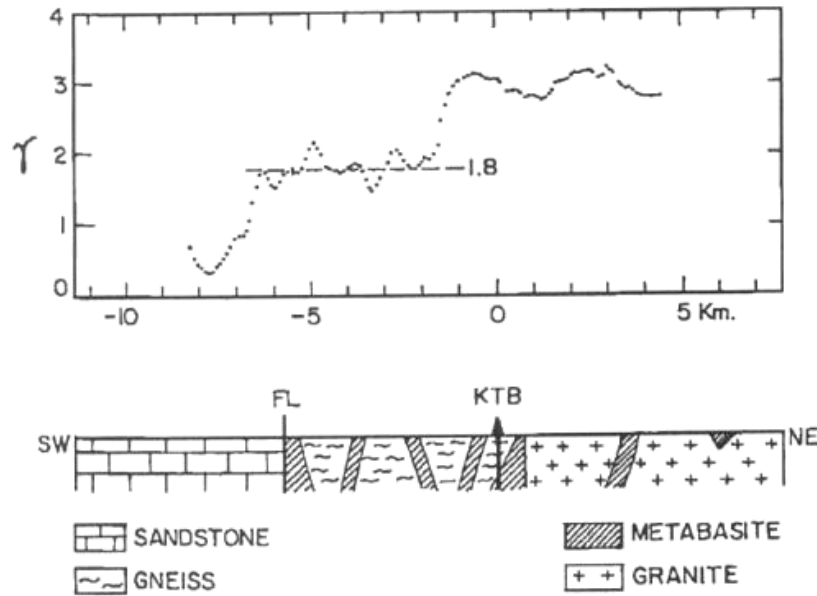


Fig. 4: Variation of scaling exponents with lithology found from aeromagnetic data over the KTB (Maus and Dimri, 1995).

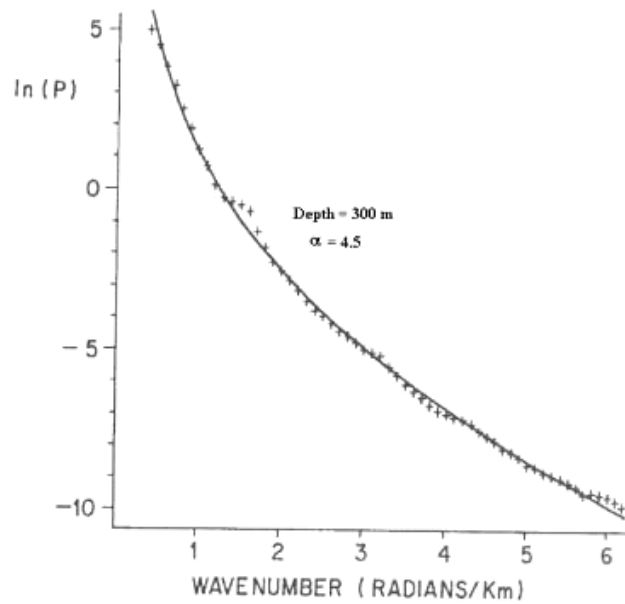


Fig. 5: Calculation of scaling exponent and depth values from aeromagnetic data over the Island of Hawaii (after Maus and Dimri, 1996).

sedimentary basin depth to magnetic basements is established as 1400 m from the seismic refraction surveys and individual magnetic anomalies modeling. The assumption of white noise source distribution result in depth estimation of 1100 m and 2400 m for the Wollastone Lake and Athabasca sedimentary Basin, respectively whereas depth values found from scaling spectral method (scaling exponent -3) are in agreement with seismic refraction studies. On the other hand Maus and Dimri (1996) calculated the scaling exponent -2.2 for the first area (Wollaston Lake) constraining the depth equivalent to flight altitude height and used the values of scaling exponent to calculate the depth values for the second study area (Athabasca Sedimentary Basin) for half space model and found depth values close to the seismic reflection studies (Fig. 2) whereas depth estimation for white noise distribution were overestimated. The fits for different depth values is shown in Fig. 2 for curve (a) for the constant and scaling exponent found from Wollaston Lake area (curve b). A depth value of 1.7 km is more suitable (Maus and Dimri, 1996). The gridding of magnetic data by using scaling information results in smoothing of the data close to the realistic data as compared to uncorrelated distribution (Pilkington *et al.*, 1994). Maus and Dimri (1996) applied the scaling spectral method to the gravity survey of the Paradox Basin Region in south – eastern Utah. The area was earlier study by the Pawlowski and obtained depth values of anomalous sources as 5 and 54 km using Spector and Grant Method whereas application of scaling spectrum method indicate dominance of scaling properties of source distribution (Fig. 3). The high values of scaling exponent indicate long range dependency of susceptibility distribution (Maus and Dimri, 1996). Maus and Dimri (1995) applied the method to the aeromagnetic data of the KTB region and found depth value of 61m close to the average flight altitude of 61.7 m. The different values of scaling exponents for different geological units were found from the aeromagnetic data over the KTB (Fig. 4) (Maus and Dimri, 1995).

Fedi *et al.* (1997) have shown the inherent power law relation of power spectra of magnetic field. They found the unique scaling exponent -2.9 from aeromagnetic spectra close to -3 (Gregotski *et al.*, 1991; Pilkington and Todoeschuck, 1993; Pilkington *et al.*, 1994). In case of synthetic example of two layer assemblage of sources at shallower and deeper depths, shallower depth values found by scaling method is close to the true assumed depths whereas deeper depth values are under estimated (Fedi *et al.*, 1997). The depth values calculated from the non corrected power are over estimated in both the cases. The application of scaling spectral method to the magnetic data of Matonipi Lake, Quebec and Tertiary volcanic lava in Central America have shown two layer and one layer assemblage of sources, respectively. This two layer and one layer case is in confirmation of large and short anomalies in Matonipi Lake area and short wavelength anomalies in Central America map.

Maus and Dimi (1996) applied the half space model with scaling properties to the aeromagnetic data of the Island of Hawaii and found depth values approximately equal to the depth of survey terrain clearance (Fig. 5). The found values of the scaling exponents is high compare with average values of -3 derived by Gregotski *et al.* (1991) from aeromagnetic survey of the North American Continent.

The spectral and scaling spectral methods are applicable to stationary gravity/magnetic data whereas in real field situation gravity and magnetic data is non stationary in nature. Therefore Bansal and Dimri (1999, 2001, 2005) suggested the division of long nonstationary profiles into piecewise stationary profiles by using the Wiener filter theory and technique is called optimum gate length. The technique

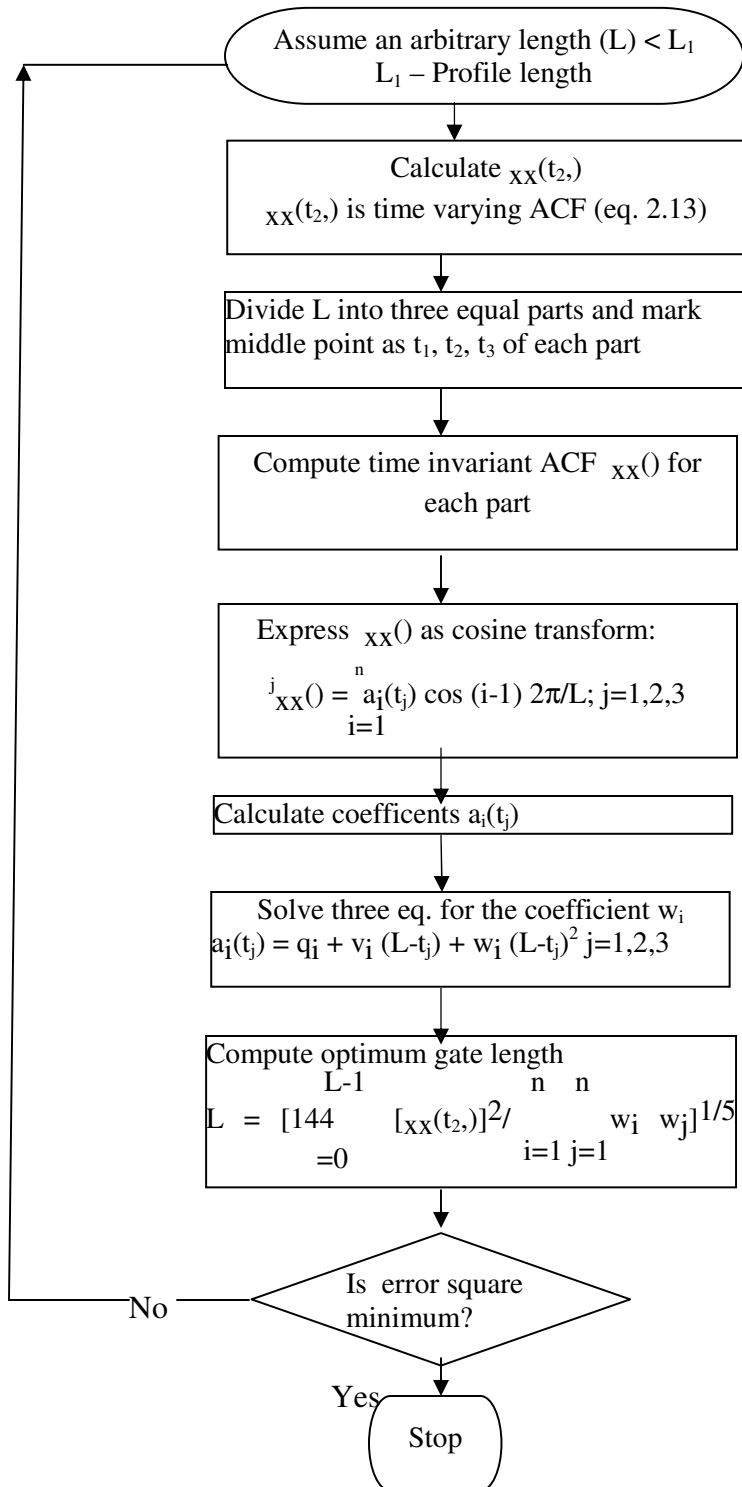


Fig. 6: A flow chart showing the calculation of optimum gate length (after Bansal and Dimri, 2005).

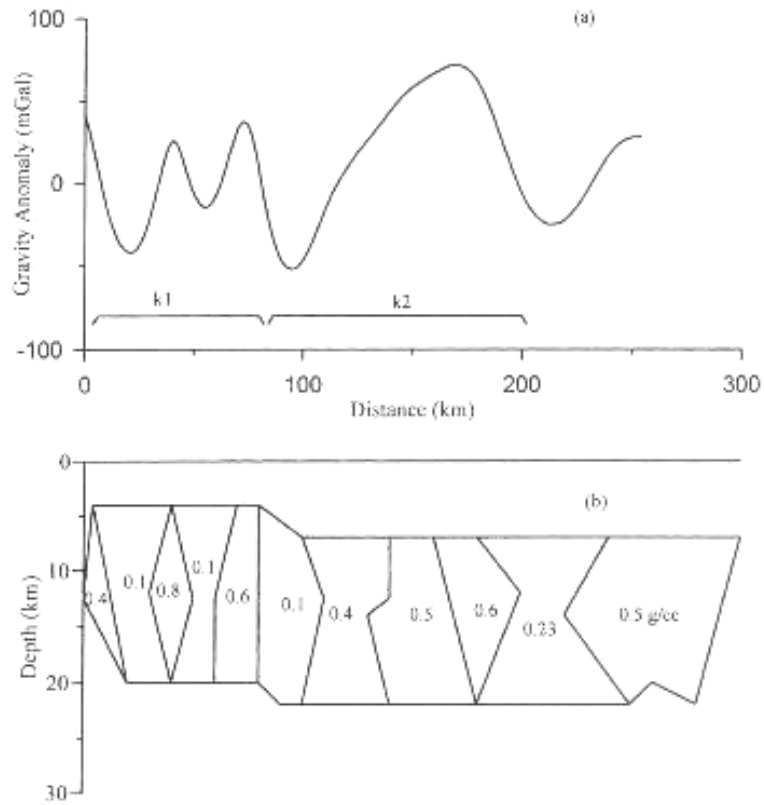


Fig. 7: (a) Synthetic gravity profile and (b) the assumed subsurface model. K1 and k2 indicate optimum gate length (Bansal and Dimri, 2001).

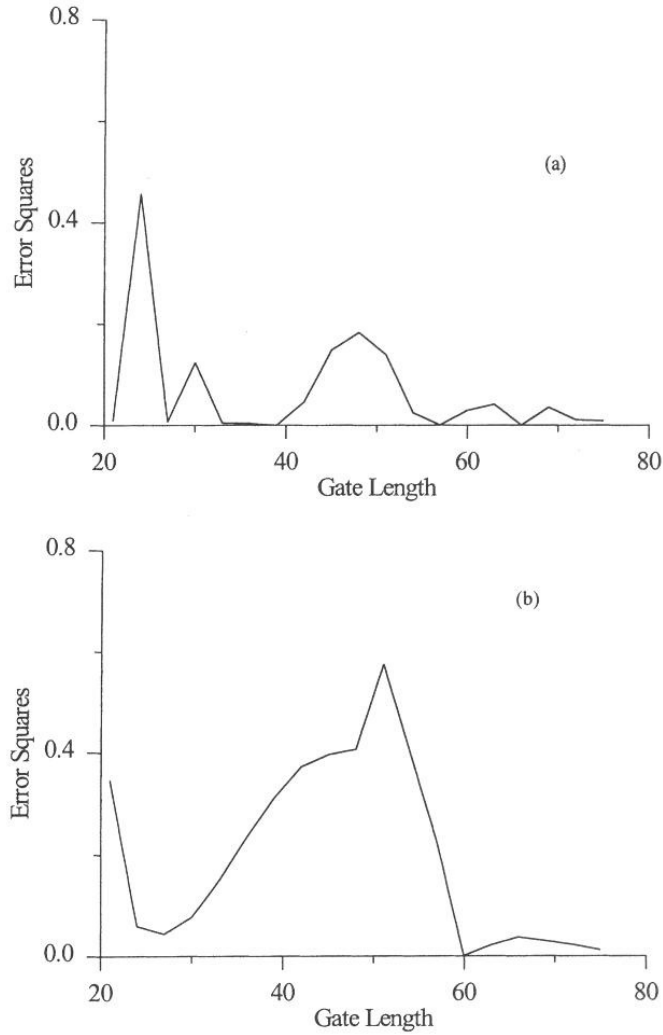


Fig. 8: Estimation of optimum gate length for (a) k1 and (b) k2 piecewise stationary sub-profiles. The minimum error square for k1 and k2 are found at 39 and 60 points corresponding to the length of 78 and 120 km since sampling interval is 2 km (Bansal and Dimri, 2001).

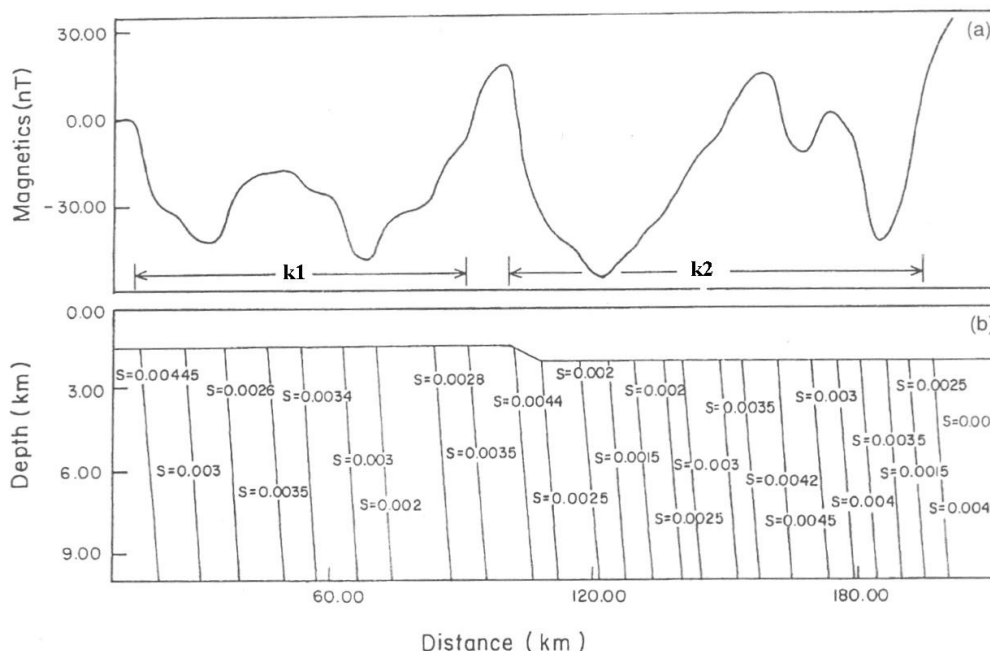


Fig. 9: (a) Synthetic magnetic profile generated for an assemblage of bodies with varying susceptibility(s) in cgs units (b). The found two optimum gate lengths were shown as k1 and k2 (after Bansal and Dimri, 2005).

was earlier developed for seismic traces by Wang (1969). The optimum gate length is selected in such a way that the error between the estimated and true time-varying autocorrelation function is minimum and thus stationarity is maintained in the computed length. The technique of dividing non-stationary gravity and magnetic profiles is consists of following steps:

- ◆ First, assume a small reasonable length of the profile.
- ◆ Divide the assumed length into three parts and mark the middle of each part.
- ◆ Calculate the time-invariant autocorrelation function for each part.
- ◆ Write these autocorrelation functions in cosine transform.
- ◆ Calculate the coefficients of cosine transform.
- ◆ Expand these coefficients in Taylor-series upto second term and calculate the Taylor coefficients.
- ◆ Calculate the time- varying auto correlation function, $\phi_{xx}(t_2, \tau)$ from following equation :

$$\phi_{xx}(t_2, \tau) = \frac{1}{L} \sum_{-L/2}^{L/2} x(t+t_2 + \frac{\tau}{2})x(t+t_2 - \frac{\tau}{2}) \quad (3)$$

Where $t_2 = L/2$

- ◆ Compute the gate length as:

$$L = 144 \left[\sum_{\tau=0}^{L-1} \phi_{xx}(t_2, \tau)^2 \sum_{i=1}^n \sum_{j=1}^n w_i w_j \right]^{1/5} \quad (4)$$

where

- ◆ $\phi_{XX}(t_2, \tau)$ is time-varying autocorrelation function,
- ◆ w_i, w_j are Taylor coefficients.
- ◆ Calculate the error square between the assumed and calculated length.

If the error square between the assumed and computed length is more, then assume a new value of length of the profile and again compute the gate length by above mentioned procedure. Repeat the whole process until a minimum error square is reached.

After selecting the optimum gate length for the first subsection, repeat the procedure for the remaining profile until whole of the profile is covered. While choosing the optimum gate length one should preserve the wavelength of anomaly. The anomaly of a sub-profile should not be cut in between i.e. the length of section should not be less than the wavelength of anomaly. The procedure of calculating the optimum gate is also presented in Fig. 6. The optimum gate length were further used to calculate depth values from scaling spectral method (Bansal and Dimri, 1999, 2001, 2005). This scheme of two steps is tested on the synthetic gravity (Bansal and Dimri, 2001) and magnetic profiles (Bansal and Dimri, 2005). The synthetic gravity profile was generated for two sets of assemblages of bodies: one shallower with high density contrast and the other deeper with less density contrasts (Fig. 7) (Bansal and Dimri, 2001). The application of optimum gatelength technique results in division of two piece-wise stationary profiles marked as k1 and k2 of length 78 km and 120 km in Fig. 7. The optimum gate length is corresponds to the minimum error square between the assumed and achieved gate length (Fig. 8). The depth values were calculated from these piecewise stationary profiles by applying the scaling spectral approach. The comparison of computed and assumed depth values were presented in Table 2. From the table 2 it can be seen that computed depth values are close to the assumed depth values. A synthetic magnetic profile were generated for an assemblage of sources with top at a depth of 1.5 and 2.0 km extended down upto 30 km for susceptibility distribution shown in Fig. 9 (Bansal and Dimri, 2005). The optimum gate length technique divided it into two stationary sub-profiles of lengths 75 and 93 marked as k1 and k2 in Fig. 9. The depth values calculated from scaling spectral method using maximum entropy method were found as 1.5 km and 1.8 km corresponding to k1 and k2, respectively are close to the assumed depth value of 1.5 and 2.0 km (Bansal and Dimri, 2005). Bansal and Dimri (1999, 2001, 2005) further applied this scheme to real gravity and magnetic data along Nagaur – Jhalawar and Jaipur – Raipur transect. They found calculated depth values are close to the depth values found from the seismic methods.

Table-2: Comparison of depth values calculated from piece stationary sub profiles (k1 and k2) using scaling spectral method and true assumed depths (Bansal and Dimri, 2001).

k1		k2	
Assumed Depth (km)	Calculated Depth (km)	Assumed Depth (km)	Calculated Depth (km)
4	3.8	7	6.6
20	---	22	23.9

Conclusions

Following conclusions can be made about the use of scaling spectral method for calculating depth values from scaling spectral method:

1. The scaling distribution of the sources is close to the realistic distribution of the sources.
2. The depth estimations of anomalous sources from the scaling spectrum method are close to the real values whereas uncorrected power spectrum results in overestimation of depth values.
3. The power spectrum corresponding to lower wavenumbers may be dominated by the scaling properties rather than depth information.
4. The calculation of scaling exponents and depth from the field data are inter-related. A higher value of scaling exponent results in lower values of depth and vice versa. Information from the boreholes can be used as preliminary information.
5. The values of scaling exponents may be anisotropic different for horizontal and vertical direction.
6. The values of scaling exponents may vary with depth.
7. The information about the scaling parameter is useful for gridding the data, deriving the lithology and source properties.
8. The longer profiles and larger areas may contain non-stationary gravity and magnetic data. Therefore before applying the scaling spectral method data should be divided into piece-wise stationary data sets.

Acknowledgements: We are thankful to management of NGRI for granting permission for publishing this work and Mr. K. K. Babu for useful discussion.

References

Bansal, A. R. and Dimri, V. P. (1999) Gravity evidence for mid crustal domal structure below Delhi fold belt and Bhilwara super group of Western India. *Geophys. Res. Letts.*, v. 26(18),pp. 2793-2795.

Bansal, A. R. and Dimri, V. P. (2001) Depth estimation from scaling power spectral density of nonstationary gravity profile, *Pure appl. Geophys.*, v. 158, pp. 799-812.

Bansal, A. R. and Dimri, V. P. (2005) Depth determination from non-stationary magnetic profile for scaling geology. *Geophys. Prosp.*, v. 53, pp. 399-410.

Bhattacharyya, B. K. (1966) Continuous spectrum of the total magnetic Field anomaly due to the Rectangular Prismatic Body. *Geophysics*, v. 31, pp. 97-121.

- Connard, G. Couch, R. and Gemperle, M. (1983) Analysis of aeromagnetic measurements from the Cascade Range in Central Oregon. *Geophysics*, v. 48, pp. 376-390.
- Cowan, D. R. and Cowan, S. (1993) Separation filtering applied to aeromagnetic data. *Exploration Geophysics*, v. 24, pp. 429-436.
- Feder, J. (1988) *Fractals*. Plenum Press, New York. 283p.
- Fedi M., Quarta T. and Santis A.D. (1997) Inherent power-law behavior of magnetic field power spectra from a Spector and Grant ensemble. *Geophysics*, v. 62, pp. 1143-1150.
- Garcia-Abdeslem, J. and Ness, G.E. (1994) Inversion of the power spectrum from magnetic anomalies. *Geophysics*, v. 59(3), pp. 391-401.
- Gregotski, M. E., Jensen, O. G. and J. Arkani- Hamed (1991) Fractal stochastic modeling of aeromagnetic data. *Geophysics*, v. 56, pp. 1706-1715.
- Hahn A., Kind E.G. and Mishra D.C. (1976) Depth estimation of magnetic sources by means of Fourier amplitude spectra. *Geophysical Prospecting*, v. 24, pp. 287-308.
- Hildenbrand T. G., J. G. Rosenbaum and J. P. Kauahikaua (1993) Aeromagnetic study of the Island of Hawaii. *J. Geophys. Res.*, v. 98, pp. 4099-4119.
- Leonardi, S. and Kumpel, H. J. (1998) Variability of geophysical log data and the signature of crustal heterogeneities at KTB. *Geophys. J. Int.*, v. 135, pp. 964-974.
- Maus S. and Dimri V.P. (1995) Potential field power spectrum inversion for scaling geology. *J. Geophysical Research*, v. 100, pp. 12605- 12616.
- Maus S. and Dimri V.P. (1996) Depth estimation from the scaling power spectrum of potential field? *Geophysical J. International*, v. 124, pp. 113-120.
- Maus, S. and Dimri, V.P. (1994) Scaling properties of potential fields due to scaling sources. *Geophys. Res. Lett.*, v. 21(10), pp. 891-894.
- Maus, S., Green, C.M. and Fairhead, J.D. (1998) Improved ocean geoid resolution from retracked ERS-1 satellite altimeter waveform. *Geophys. J. Int.*, v. 134, pp. 243-253.
- Naidu, P. S. (1972) Maximum Likelihood (ML) estimation of depth from the spectrum of aeromagnetic field. *Pure Appl. Geophys.*, v. 95, pp. 141-149.
- Naidu, P. S. (1968) Spectrum of the Potential Field due to Randomly Distributed Sources. *Geophysics*, v. 33, pp. 337-345.
- Naidu, P.S. and Mathew, M.P. (1998) *Analysis of geophysical potential fields, A digital signal processing approach*. Elsevier Science publishers, Amsterdam, 298p.
- Ofoegbu, C. O. and Hein, K. (1991) Analysis of magnetic data over part of the Younger Granite Province of Nigeria. *Pure Appl. Geophys.*, v. 136, pp.173-189.
- Pawlowski, R. S. (1994) Green's equivalent- layer concept in gravity band-pass filter design. *Geophysics*, v. 59, pp. 69-76.
- Pedersen, L. B. (1991) Relations between potential fields and some equivalent sources. *Geophysics*, v. 56, pp. 961-971.
- Pilkington, M. and Todoeschuck, J.P. (1990) Stochastic inversion for scaling geology. *Geophysical J. International*, v. 102, pp. 205-217.
- Pilkington, M. and Todoeschuck, J.P. (1993) Fractal magnetization of continental crust. *Geophysical Research Letters*, v. 20, pp. 627- 630.
- Pilkington, M. and Todoeschuck, J.P. (1995) Scaling nature of crustal susceptibilities. *Geophysical Research Letters*, v. 22, pp. 779-782.
- Pilkington, M., Gregotski, M.E. and Todoeschuck, J.P. (1994) Using fractal crustal magnetization models in magnetic interpretation. *Geophysical Prospecting*, v. 42, pp. 677-692.
- Shiomi, K., Sato, H. and Ohtake, M. (1997) Broad- band power-law spectra of well-log data in Japan. *Geophys. J. Int.*, v. 130, pp. 57-64.
- Spector, A. and Grant, F.S. (1970) Statistical model for the interpreting of aeromagnetic data. *Geophysics*, v. 35, pp. 293-302.
- Treitel, S., Clement, W.G. and Kaul, R.K. (1971) The spectral determination of depths of buried magnetic basement rocks. *Geophysical Journal of the Royal Astronomical Society*, v.24, pp. 415-428.
- Wang, R.J. (1969) The determination of optimum gate lengths for time varying Wiener filtering. *Geophysics*, v. 34(5), pp. 683-695.
- Zhou, S. and Thybo, H. (1998) Power spectra analysis of aeromagnetic data and KTB susceptibility logs, and their implication for fractal behavior of crustal magnetization. *Pure and Applied Geophysics*, v. 151, pp. 147-159.

About the author



Dr. Abhey Ram Bansal is a scientist E1, National Geophysical Research Institute, Hyderabad. His research interests are Fractals in Geophysics, Signal Processing, Gravity and Magnetic Method and Statistical Seismology. He obtained M. Tech (Applied Geophysics) in 1994 from Kurukshetra University, Kurukshetra and Ph.D. (Geophysics) in 2001 from Osmania University, Hyderabad. Dr. Bansal received several awards such as Krishnan Gold Medal – 2008, UKIERI Fellowship - 2007, National Mineral Award 2005, BOYSCAST Fellowship -2001. He is Associate Fellow A. P. Akademy of Sciences and Member, National Academy of Sciences, India. He published more than eighteen papers in reputed national and international journals.